



AIAA-2002-2822

**Control of a High-Speed Impinging Jet using a
Hartmann-Tube based Fluidic Actuator**

Mo Samimy, Jeff Kastner, and Marco Debiasi
The Ohio State University
Department of Mechanical Engineering
Columbus, OH 43210
USA

1st AIAA Flow Control Conference
24-26 June 2002/ St. Louis, MO

Control of High-Speed Impinging Jets using Hartmann Tube Fluidic Actuators

M. Samimy^{*}, J. Kastner[†], and M. Debiasi[‡]
 Gas Dynamics and Turbulence Laboratory
 The Ohio State University
 Columbus, Ohio 43210
 AIAA 2002-2822

We report preliminary results obtained using Hartmann tube fluidic actuators (HTFA) and steady injection to explore the effects of forcing frequency in controlling the behavior of a high-speed impinging jet. One or two actuators were used to force the flow produced by an axisymmetric, Mach 1.3 ideally expanded jet impinging upon a plate located 4 jet diameters downstream. The impingement tone frequency was 5.3 kHz. A weaker resonance at the same frequency was obtained by using a baffle that reduced the communication and thus coupling between the acoustic and flow fields. The three actuators used had the same mass flow rate, but frequencies at 0 (steady injection), 5.4 (near the impingement tone of 5.3 kHz), and 12 kHz. Measurements were performed to characterize the near- and far-field acoustics of the unforced and forced jets. The very preliminary results show that while a single actuator does not seem to have sufficient authority, two actuators separated 180° in the azimuthal plane can significantly modify the flow. The flow and acoustic fields, especially for the forced cases, are three dimensional, which make the interpretation of the results quite challenging. A cursory analysis of the data seems to suggest that: (1) each type of actuator behaves in a similar fashion in both strong and weak resonance cases; (2) the steady injection forcing and high frequency (12 kHz) forcing behave similarly in either suppressing the impingement tone or significantly weakening it, but raise the broadband acoustic level around the impingement tone; (3) the low frequency (5.4 kHz) forcing suppresses the impingement tone, but gives less rise to the broadband noise; and (4) both the high frequency and low frequency forcing leave their imprint at the forcing frequency. The low frequency forcing is very close to the impingement tone, therefore, it is a close call whether the impingement tone is suppressed or not at this forcing frequency. An audible change in the tone during experiment however confirms that the impingement tone is suppressed and energy is put into the forcing frequency.

1. Introduction

Impinging jets have many practical applications and, similar to flows over a cavity, are characterized by self-sustained oscillations (e.g., Ho and Nosseir, 1981; Tam and Ahuja, 1990). In these flows there is a strong coupling between flow and acoustic fields and a natural feedback mechanism drives part of

the system's mechanical energy into specific frequencies. In general, this occurs when large-scale structures in the shear layer convect downstream and, upon interaction with a solid boundary, scatter acoustic waves that propagate upstream to the shear layer receptivity region. Here the acoustic waves force the generation of new structures at the same frequency. The system thus resonates at a well-defined frequency and its harmonics, in general, and the corresponding strong pressure fluctuations and radiated noise can cause significant damage to nearby objects. In the case of subsonic jets, the acoustic waves propagate upstream both within the jet column

^{*}Professor, Associate Fellow AIAA

[†]Graduate Student, member AIAA

[‡]Post Doctoral Researcher, member AIAA

and outside it. For supersonic flows the acoustic waves can only excite the shear layer at the nozzle exit by traveling outside of the jet column (Varnier and Raguenet, 2002).

The exhaust of STOVL (or VTOL) aircraft hovering close to the ground gives a typical example of impinging jet. In this case an additional problem is the loss of lift associated with the high entrainment of ambient air into the jet induced by well-organized coherent structures due to the resonance condition (Alvi et al., 2000; Elavarasan et al., 2001).

Clearly the attenuation or elimination of the impinging jet feedback mechanism would be beneficial in many applications. In principle, this can be done by disrupting the ability of the upstream propagating waves to excite the flow at the nozzle exit. Elavarasan et al. (2001) demonstrated that the use of a simple passive device like a baffle placed near the nozzle exit is effective in interrupting the upstream propagation of the acoustic waves. The use of active control is more attractive due to its potential flexibility and adaptation. Since active control entails the use of some energy input to modify the flow field, in this case it is usually preferred to act on the receptivity region for an effective and efficient delivery of energy. Examples of active control work include the use of a coflow (Sheplak and Spina, 1994), microjets (Alvi et al., 2000), or Hartmann tubes (Stanek et al., 2000/2001/2002; Raman et al., 2001), all of which have been shown to be successful in reducing the resonant tones.

Wiltse and Glezer (1998) introduced the idea of high frequency forcing as a means to suppress the growth of large-scale structures by channeling energy to small-scale dissipating structures. They demonstrated the concept by using piezoelectric actuators to excite a low Reynolds number jet at a frequency corresponding to the inertial subrange. Cain (in Raman et al., 2000) suggested that this method could effectively control resonant flow phenomena. Successive experiments carried out by Stanek et al. (2000 and 2001) on cavity

flow and by Raman et al. (2001) on supersonic, rectangular impinging jets demonstrated that the use of Hartmann tubes for high-frequency, high-amplitude excitation reduces the resonant tone. A new interpretation of the high frequency forcing has been very recently offered by Stanek et al. (2002). Note that the work of Wiltse and Glezer was in a flow with no resonance, while the other works referenced in this paragraph were all in flows with resonance.

The purpose of the current work is to further explore the potential and nature of high frequency and amplitude excitation in both resonance and non-resonance (or perhaps strong and weak resonances) in a Mach 1.3 ideally expanded axisymmetric impinging jet. In this study the effect of single and dual Hartmann tube fluidic actuator (HTFA) configurations with both low frequency and high frequency but the same mass flow rate, as well as steady injection with the same mass flow rate as the HTFAs, were used in both strong and weak resonance cases.

2. Experimental Setup

2.1 Jet facility

All the experiments were performed in the optically accessed anechoic chamber of the Gas Dynamics and Turbulence Laboratory (GDTL) at The Ohio State University. This facility, described more in detail in Kerechanin et al. (2000), complies with ANSI Standard S12.35. The nozzle used in the experiments was an axisymmetric Mach 1.3 nozzle with an exit diameter D of 25.4 mm (1 inch). The converging section of the nozzle was designed using a fifth order polynomial while the diverging section was designed using the method of characteristics for uniform exit flow. A straight extension of 8.5 mm (0.33 in) long incorporating 6x4 mm openings for the injection of the HTFA flow was added after the diverging section. The Reynolds number of the jet based on the jet diameter is 1.06×10^6 .

The air was supplied to the nozzle by two four-stage compressors. The air was filtered, dried, and stored at 16.5 MPa in two high-capacity tanks. The air was conditioned in a stagnation chamber before entering the nozzle. The total pressure in the stagnation chamber was controlled by a Fisher Type 667-D control valve capable of maintaining the pressure within 0.3 psi of the desired value for operating the nozzle at ideally expanded conditions.

The impinging plate consisted of a 305 mm (12") diameter disk with 31.75 mm (1¼") thickness mounted perpendicular to the jet axis on a stand that allowed the distance, ℓ , between the plate and the nozzle exit to be varied. This allowed the control of both the amplitude and frequency of the impinging tone that depends on ℓ . A schematic of this arrangement is given in Figure 1.

In order to weaken the resonance, a rectangular baffle of 82x70 mm that had a semi-circular cutout of 14 mm in radius, a geometry similar to that used by Elavarasan et al. (2001), was placed 6.3 mm (¼ in) downstream of the jet nozzle exit in some of the experiment. In all the experiments the baffle was placed at $\theta = 0^\circ$ side.

2.2 Hartmann Tube Fluidic Actuator (HTFA)

HTFA is a very attractive device in high-speed flow control due to its capability of generating high amplitude and high frequency pulsating flows (Raman et al. 2000; Raman and Kibens 2001; Kastner and Samimy 2002). In its simplest form, a Hartmann tube consists of an underexpanded jet issuing from a nozzle and entering a coaxial resonance tube of the same diameter as the nozzle. When the entrance of the tube is located within a compression cell of the underexpanded jet, a cyclical flow field, within the tube and out of the nozzle/tube system, is established (Hartmann and Trolle, 1927; Hartmann, 1939). In the first part of the cycle, air is entrained into the tube while in the remainder of the cycle the overpressure created in the tube

ejects the entrained air (Brocher et al., 1970). There is a strong coupling between the flow and acoustic field in a Hartmann tube.

The use of Hartmann tubes as fluidic actuators for active flow control was first introduced by Raman et al. (2000) and Raman and Kibens (2001). When used in this fashion a shield is placed between the nozzle and the tube in order to direct the ejected flow in a specified direction. While most of the past research on Hartmann tubes had focused on the temperature and pressure within the resonance tube, more information has been obtained over the past few years about the flow field between the nozzle and resonance tube. Recently the focus has shifted to the flow field generated by HTFA (Raman et al., 2001; Kastner and Samimy, 2002). Planar flow visualization by Kastner and Samimy showed the flow exited a HTFA is rich in vortical structures.

The frequency of the HT can be estimated using a simple quarter wave frequency equation,

$$f = \frac{a_o}{4L} \quad (1)$$

where L is the depth of the tube and a_o is the speed of sound. It is known that this equation is much less accurate in shorter tubes (higher frequencies). Furthermore, it has been shown that the use of stepped or conical tubes, which were first introduced by Sprenger (1954), increases the frequency of the pulsating flow (Kawahashi et al, 1984).

Figure 2 shows a schematic drawing of a typical HTFA used in the present study. The axisymmetric, converging nozzle, on the left, has an exit diameter $d = 4$ mm. A static tap placed at the nozzle exit was used to verify the required underexpanded operating conditions. Various resonant tubes, on the right of Fig. 2, with different depth and internal geometry could be installed at a distance $\Delta X = 6$ mm (i.e. $1.5d$) from the nozzle. A cylindrical tube with depth $L = 8$ mm was used to obtain a tonal frequency of 5.4 kHz, closely matching the impinging tone, a tube with four steps (of

diameter from 4 mm to 1 mm and each having length 2 mm) and the same overall depth gave a frequency of 12 kHz while a plugged tube ($L = 0$) was used to create steady injection of the same mass flow rate of the HTFA. A shield placed between the nozzle and the tube directed the pulsating flow into a small rectangular opening (6 mm x 4mm) on the shield lined up with a same size opening in the straight extended section of the main jet nozzle. The arrangement ensured injection of the HTFA pulsating flow perpendicular to the main flow. Two actuators were placed in the jet azimuthal plane respectively at $\theta = 0^\circ$ and 180° and were operated independently. This allowed operation of one or both actuators at a time.

2.3 Diagnostics

Near-field pressure measurements and far-field acoustic measurements were conducted as well as velocity measurements at the exit of a HTFA. Near-field measurements were made using an Endevco Model 8514-10 dynamic pressure transducer with frequency response up to 100 kHz. Due to a 40 kHz resonance caused by the cap covering the transducer, data will be presented only for frequencies up to 30 kHz. The transducer was located 50.8 mm (2") downstream of the jet nozzle exit at a radial distance $r = 19$ mm ($3/4$ ") from the jet axis forming an angle $\phi = 21^\circ$ with respect to the jet axis (see Fig. 1). The signal from the pressure transducer was amplified using an Ectron (Model 563F) signal conditioner. For far-field measurements two 6.35 mm ($1/4$ in) Bruel and Kjaer Model 4135 microphones connected to Bruel and Kjaer Model 2633A preamplifiers were located in the jet longitudinal plane at polar angles $\phi = 80^\circ$ and 90° and distance $r = 76$ cm (see Fig. 1). The microphone signals were amplified by a Bruel and Kjaer Nexus conditioning amplifier and band pass filtered from 20 Hz to 100 kHz before sampling at 200 kHz using a National Instruments A/D acquisition board. The microphones were calibrated before each set of experiments using a Bruel and Kjaer

Model 4231 calibrator. The acquired data were processed using Matlab codes. Since the amplitude of the impinging tone was larger for the microphone location of 80° , but qualitatively the same as that of the microphone at 80° , we limit our presentation to the data obtained at this location.

Successful control of high-speed flows would require high authority, which mean high velocities at the exit of the actuator. In order to obtain velocity at the actuator exit (i.e. at the point of injection into the jet), a hot-film probe (TSI Model 1201) was used. The probe was calibrated using a converging nozzle at known pressure ratios. The data for the hot film was sampled at 40 kHz.

3. Results

3.1 Hartmann Tube Fluidic Actuator

Before the discussion of the effect of actuation on the impinging jet, it is of paramount importance to describe the characteristics of the HTFA used in this study. Both far-field acoustic measurements and dynamic velocity measurements were performed at the exit of a HTFA. Detailed assessment of the frequency content of HTFA was obtained by performing far-field acoustic measurements similar to those presented by Kastner and Samimy (2002). The far-field spectra of the three actuators used in the current experiment mounted on the Mach 1.3 impinging jet, but with the jet off, are presented in Figure 3. The actuators include a low frequency, a high frequency, and a steady injection actuators. The actuator was operated in the underexpanded regime at M_j of 1.4 in all three cases. For this condition the mass flow rate of each actuator was approximately 3% of the main jet's mass flow rate. Figure 3(a) shows that the low-frequency actuator has a strong peak at 5.4 kHz with three harmonics. In contrast, a single strong peak at 12 kHz characterizes the high-frequency actuator, Fig. 3(b). The steady injection case, Fig. 3(c) does not possess any tonal frequency.

Hot-film velocity measurements were performed at the output flow of a HTFA. Due to the relatively low frequency response of the hot film (up to 9 kHz) a lower frequency HTFA with a tube depth $L = 18$ mm and tonal frequency of 3.5 kHz was used to keep the frequency less than half the frequency response of the hot film. The far-field acoustic spectrum for the 18 mm tube is presented in Fig. 4(a), which reveals a rich spectral content. Comparison with the corresponding velocity spectrum shown in Fig. 4(b) clearly indicates that the velocity tonal content is very similar to the far-field acoustic tonal content. Comparison of the velocity-fluctuation spectrum at the exit of HTFA shown in Fig. 4(b) and the far-field acoustic spectrum for steady injection ($L = 0$) shown in Fig. 3(c), further corroborates the strong coupling between acoustic and flow fields in a HTFA. Based on these results we can infer a similar behavior for the low frequency (5.4 kHz) and high frequency (12 kHz) HTFAs used in the current experiments, as well.

The HTFA with a tube depth of 18 mm has significantly higher velocity fluctuations compared to the steady injector, which is not surprising considering spectra shown in Fig. 4(b). The mean velocity for the steady injector was 170 m/s and the fluctuation intensity was 2.5% while for the 18 mm tube injector the mean velocity was reduced to 140 m/s and the fluctuation intensity was increased to 18%. Obviously, HTFAs used here are high authority actuators.

3.2 Impinging Jet Flow

With the present setup we studied two types of impinging jet flow: the first with a strong resonance, the second with a weaker resonance. The behavior of the impinging jet flow (Mach 1.3 ideally expanded) was explored without forcing while placing the plate at various distances ℓ relative to the nozzle exit. Figure 5 presents the resonant frequency as a function of the distance ℓ varying between 45 mm and 220 mm from the nozzle exit. For each plate location, the two largest-amplitude tones recorded by the

microphone located at $\phi = 80^\circ$ are shown. The solid lines in the figure represent the resonant frequency obtained using the simplified version of the formula originally proposed by Powell (1953)

$$N = \frac{f\ell}{U_c} + \frac{f\ell}{a_o} \quad (2)$$

where N is an integer, f is the resonant tone frequency, ℓ is the distance between the nozzle exit and the impinging plate, U_c is the convective velocity of the turbulence structures, and a_o is the speed of sound at ambient temperature. The convective velocity was chosen to be 265 m/s, which provided a good fit to the experimental data. This is close to the value of 270 m/s average convective velocity measured in the same jet but without impingement plate by Thurow et al. (2002). In reality the convective velocity varies with impinging plate location, which should be taken into account in using Equation 2.

The plate location at $\ell = 105$ mm, with a strong resonance at 5.3 kHz almost matching the fundamental frequency of the HTFA at 5.4 kHz, was chosen for the baseline resonant flow. This is indicated by two larger dots in Fig. 5. Figures 6(a) and 6(b) show the near- and far-field spectra for this baseline case. The resonant tone frequency at 5.3 kHz corresponds to a Strouhal number, fD/U_j , of 0.33. The first harmonic of the resonance tone at 10.6 kHz is strong both in the near- and far-field. Using the baffle described in § 2.1 created the case of weak resonance. The near and far-field spectra for this case are also presented in Figures 6(c) and (d) that exhibit a weaker tone without any detectable harmonics. The use of the baffle induces a shift of the tone to a slightly higher frequency (5.6 kHz), a phenomenon observed in other work as well (Elavarasan et al, 2001). For convenience, Figs. 6(a)-(d) will be shown again for comparison with the corresponding cases with actuation.

3.3 Forcing of the baseline Impinging Jet

We first present the results obtained forcing the strong-resonance case with the steady injector, the low-frequency actuator, and the high-frequency actuator. The results for forcing using two simultaneous actuators are discussed first. Figure 7 compares the near-field pressure fluctuations obtained at $\theta = 0^\circ$ for the baseline flow with the three different actuators. Figure 7(b) shows that the steady injector significantly reduces the impinging tone. Forcing at 5.4 kHz, Fig. 7(b), slightly reduces and shifts the tone to the actuator frequency. Forcing at 12 kHz in Fig. 7(d), eliminates the impingement tone, but puts energy into the forcing frequency. There is an appreciable increase of broadband noise at and around the impingement tone for the steady injection and high frequency forcing, and to a lesser degree for the low frequency forcing.

For the same cases the near-field results in the $\theta = 90^\circ$ plane are presented in Figure 8. In general, the effect on the impinging tone is similar to that observed at $\theta = 0^\circ$. Different from the measurements at $\theta = 0^\circ$ are the appearance of a higher frequency tone at 9.8 kHz in Fig. 8(b) and by the strong harmonic of the low-frequency actuator in Fig. 8(c). In addition it should be noted that at this angle actuation does not produce the broadband increases observed at $\theta = 0^\circ$ degrees.

Figure 9 presents far-field spectra in the $\theta = 0^\circ$ plane. Steady injection, Fig. 9(b), completely eliminates the impinging tone. Forcing at 5.4 kHz in Fig. 9(c) produces a rather weak tone with a strong harmonic whose intensity is comparable to the initial impinging tone. Forcing at 12 kHz, Fig. 9(d), completely suppresses the impingement tone but produces only a weaker peak at the actuation frequency. The peaks at the actuation frequencies are in both cases comparable to the peak broadband noise. Far-field spectra at $\theta = 90^\circ$, not presented here, have similar features.

Figures 10 and 11 show the near and far-field spectra at 0° for forcing with a single HTFA. In these experiments, the single actuator was located at 0° . The use of a single actuator does not seem to significantly modify the natural behavior of the impinging jet. For all three types of actuation, the near field spectra in Figs. 10(b)-(d) are very similar with a slight enhancement of the impinging tone accompanied by the broadband noise increase already noted in Fig. 7. The far-field spectra with actuation, Figs. 11(b)-(d), are also very similar to the corresponding unactuated case shown in Fig 11(a). The near and far-field measurements with one actuator in other directions support similar conclusions.

3.4 Forcing of the baffled Impinging Jet

The effect of actuation was also studied in the case of a weaker resonance. As explained in the previous sections, this weaker resonance case was obtained by placing a baffle downstream of the nozzle exit, which produced minimal alteration of the other general characteristics of the resonant flow. With baffle the impinging tone was significantly weakened and shifted to the slightly higher frequency of 5.6 kHz in the near field, and was hardly noticeable in the far field. For the sake of simplicity in this section we restrict the presentation to the measurements obtained at $\theta = 0^\circ$.

The near field results with the use of two actuators are presented in Figure 12. The trends in the spectra with actuations are similar to those of Fig. 7. In this case the steady injector has completely eliminated the impinging tone in Fig. 12(b) and, similar to the strong resonance counterpart case, actuation at 5.4 and 12 kHz shifted the tone to the actuator frequency in Figs. 12(c) and (d). As previously observed there is an appreciable increase of broadband noise with actuation, especially in the steady injection and high frequency forcing cases. Far-field measurements, not presented here, are consistent with these results.

The behavior of a single actuator was explored by placing it on the same side of the baffle ($\theta = 0^\circ$) or opposite to it ($\theta = 180^\circ$). In the following we will simply refer to these positions as “same” and “opposite”. This will avoid confusion with the microphone position. Due to the very complex and directional nature of the near-field, we restrict ourselves to the far-field data (Figure 13), which more clearly capture some relevant characteristics of the flows. Figure 13(a) and (b) show respectively the effect of the steady injector in the same and opposite side of the baffle. Actuation in the same side, Fig. 13(a), exhibits the impinging tone and its first harmonic as well as a weaker tone at 16 kHz. When placed on the opposite side, both the tone and its harmonic disappear but a smaller peak appears at 22 kHz.

Use of the 5.4 kHz HTFA on the same side of the baffle, Fig. 13(c), produces a spectrum similar to that of Fig. 13(a), but with slightly higher peaks. The spectrum for the actuator placed on the opposite side, Fig. 13(d), is also very similar to the corresponding spectrum for the steady injector in Fig. 13(b), the most notable difference being a shift of the small peak to 20 kHz. The behavior of the 12 kHz actuator on the same side of the baffle is similar to that of the other actuators except for the reduction of the 16 kHz tone and the appearance of the first harmonic of the forcing frequency at 24 kHz. With the actuator on the opposite side the spectrum is similar to those of Figs. 13(b) and (d) except for the slightly different position of the small peak which now is at 21 kHz.

5. Conclusions

A series of experiments were designed and conducted to explore the effects of forcing frequency in an impinging jet with both a weak and a strong resonance. Hartmann tube fluidic actuators (HTFA) with zero frequency (steady injection), low frequency of 5.4 kHz (near the jet resonance frequency of 5.3 kHz), and high frequency of 12 kHz were used. All three actuators had the same mass flow rate of

approximately 3% of the jet flow. Either one or two actuators separated 180° in azimuthal direction were used to inject steady or pulsating flow at 90° to the jet/nozzle axis just upstream of the nozzle exit. A baffle was used to weaken the resonance and thus to allow forcing of the impinging jet at both strong and weak resonance cases. The impinging jet was an axisymmetric, Mach 1.3 ideally expanded jet impinging upon a plate located 4 jet diameters downstream. Measurements were performed to characterize the near- and far-field acoustic of the unforced and forced jets. The following very preliminary conclusions can be drawn.

- The flow and acoustic fields, especially for the forced cases, are three dimensional, and thus the interpretation of the results based on point measurements are quite challenging.
- A single actuator does not seem to have sufficient authority to suppress the impingement tone. In fact, it slightly enhances the impingement tone and also increases broadband noise at and around the impingement tone.
- Two actuators separated 180° in the azimuthal plane can significantly modify the flow.
- The actuators behave in a similar fashion in both strong and weak resonance cases.
- For the two actuators case:
 - The steady injection forcing and high frequency (12 kHz) forcing behave similarly: either suppress the impingement tone or significantly weaken it, but raise the broadband acoustic level around the impingement tone.
 - The low frequency (5.4 kHz) forcing suppresses the impingement tone, but does not raise the broadband noise

as much as the other two cases.

- Both the high frequency and low frequency forcing leave their imprint at the forcing frequency.

The frequency of the low frequency forcing (5.4 kHz) is very close to the impingement tone (5.3 kHz). Therefore, it is a close call whether the impingement tone in this case is suppressed or not by forcing. However, an audible change in the tone during experiment confirms that the impinging tone is suppressed and energy is put into the forcing frequency.

It should be emphasized that the results and the conclusion drawn are very preliminary. The current results will be analyzed further, additional results, specially detailed flow visualizations, will be obtained to guide us in the interpretation of the results.

Acknowledgements

The support of this research by an AFL/DAGSI grant (with Mike Stanek) is greatly appreciated.

References

- Alvi, F.S., Elavarasan, R., Shih, C., Garg, G., and Krothapalli, A., "Active Control of Supersonic Impinging Jets Using Microjets," AIAA 2000-2236.
- Brocher, E., Maresca, C., and Bournay, M.-H., "Fluid Dynamics of the Resonance Tube," *J. Fluid Mech.*, Vol. 43, Part 2, 1970, pp. 369-384.
- Elavarasan, R., Krothapalli, A., Venkatakrisnan, L., and Lourenco, L., "Suppression of Self-Sustained Oscillations in a Supersonic Impinging Jet," *AIAA J.*, Vol. 39, No. 12, December 2001.
- Hartmann, J., and Trolle, B., "A New Acoustic Generator," *J. Sci. Instr.*, Vol. 4, 1927, pp. 101-111.
- Hartmann, J., "Construction, Performance, and Design of the Acoustic Air-Jet Generator," *J. Sci. Instr.*, Vol. 16, 1939, pp. 140-149.
- Ho, C.M., and Nosseir, N.S., "Dynamics of an Impinging Jet. Part 1. The Feedback Phenomenon", *J. Fluid Mechanics*, Vol. 105, 1981, pp. 119-142.
- Kastner, J., and Samimy, M., "Development and Characterization of Hartmann Tube based Fluidic Actuators for Flow Control," AIAA 2002-0128.
- Kawahashi, M., Bobone, R., and Brocher, E., "Oscillation Modes in Single-Step Hartmann-Sprenger Tubes," *J. of the Acoustical Society of America*, Vol. 75, No. 3, 1984, pp. 780-784.
- Kerechanin, C.W., Samimy, M., and Kim, J.H., "Effects of Nozzle Trailing Edge Modifications on Noise Radiation in a Supersonic Rectangular Jet," AIAA paper 2000-0086.
- Powell, A., "On edge tones and associated phenomena", *Acoustica*, Vol. 3, 1953, pp. 233-243.
- Raman, G., Kibens, V., Cain, A., and Lepicovsky, J., "Advanced Actuator Concepts for Active Aeroacoustic Control," AIAA 2000-1930.
- Raman, G., and Kibens, V., "Active Flow Control Using Integrated Powered Resonance Tube Actuators," AIAA 2001-3024.
- Raman, G., Mills, A., Othman, S., and Kibens, V., "Development of Powered Resonance Tube Actuators for Active Flow Control," ASME FEDSM 2001-18273.
- Sheplak, M., and Spina, E.F., "Control of High-Speed Impinging Jet," *AIAA J.*, Vol. 32, No. 8, 1994, pp. 1583-1588.

Sprenger, H., "Ueber thermische Effekte in Resonanzrohren," Fed. Inst. Tech., Zurich, Vol. 21, 1954, pp. 18-35.

Stanek, M.J., Raman, G., Kibens, V., Ross, J.A., Odedra, J., and Peto, J., "Control of Cavity Resonance Through Very High Frequency Forcing," AIAA 2000-1905.

Stanek, M.J., Raman, G., Kibens, V., Ross, J.A., Odedra, J., and Peto, J., "Suppression of Cavity Resonance Using High Frequency Forcing – The Characteristic Signature of Effective Devices," AIAA 2001-2128.

Stanek, M.J., Raman, G., Ross, J.A., Odedra J., Peto, J., Alvi, F., and Kibens, V., "High Frequency Acoustic Suppression – The Role of Mass Flow, The Notion of Superposition, And The Role of Inviscid Instability – A New Model (Part II)", AIAA 2002-2404.

Tam, C.K.W., and Ahuja, K.K., "Theoretical Model of Discrete Tone Generation by Impinging Jets," J. Fluid Mechanics, Vol. 214, 1990, pp. 67-87.

Thurrow, B., Hileman, J., Samimy, M., and Lempert, W., "Compressibility Effects on the Growth and Development of Large-Scale Structures in an Axisymmetric Jet", AIAA 2002-1062.

Varnier, J., and Ragueneau, W., "Experimental Characterization of the Sound Power Radiated by Impinging Supersonic Jets," AIAA J., Vol. 40, No. 5, 2002.

Wiltse, J.M. and Glezer, A., "Direct Excitation of Small-Scale Motions in Free Shear Flows", Physics of Fluids, Vol. 10, No. 8, 1998, pp. 2026-2036.

Figures

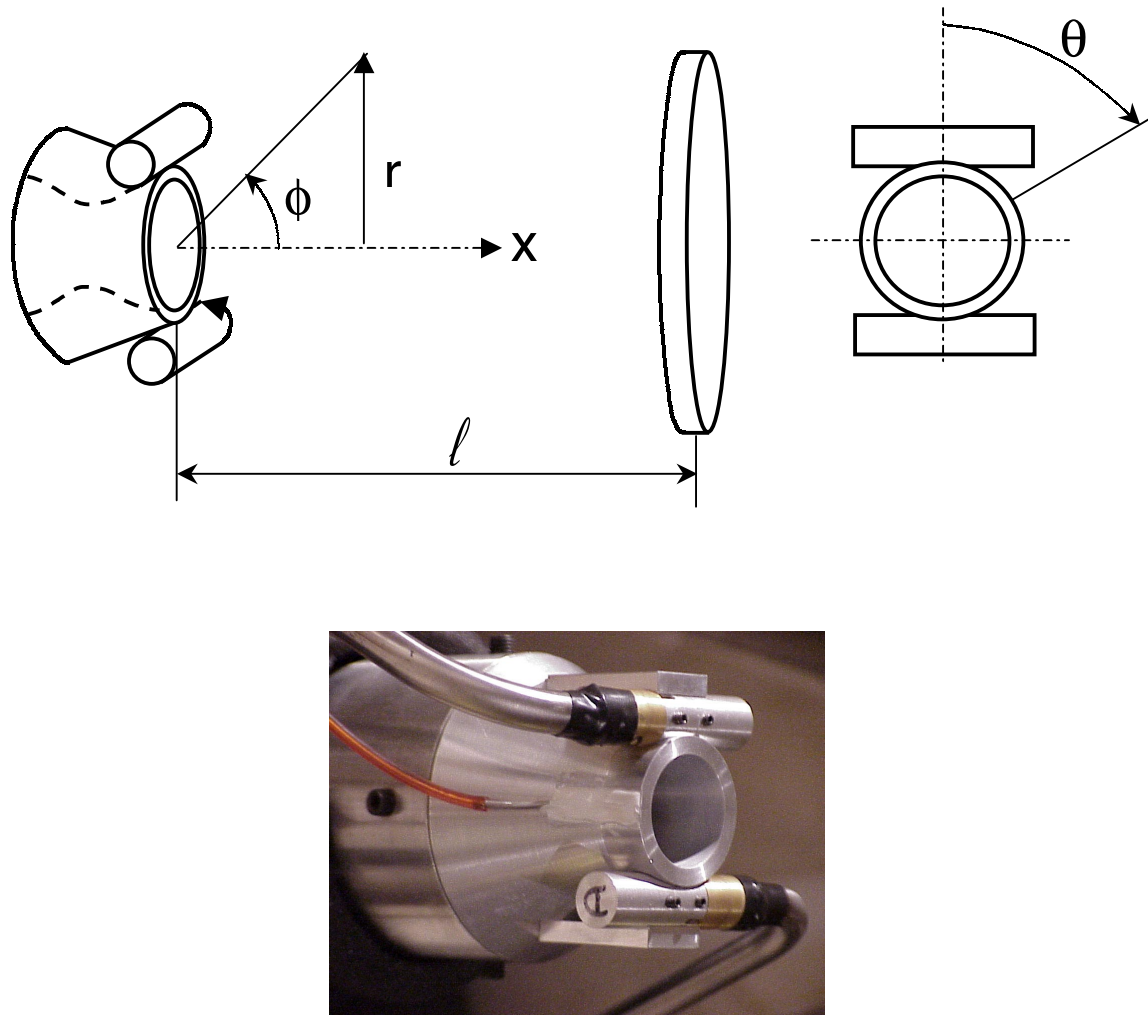


Figure 1: Schematic of the experimental setup (outlining the jet with the actuators and position of the impinging plate) (top) and a digital photograph of the Mach 1.3 nozzle with the actuators attached (bottom).

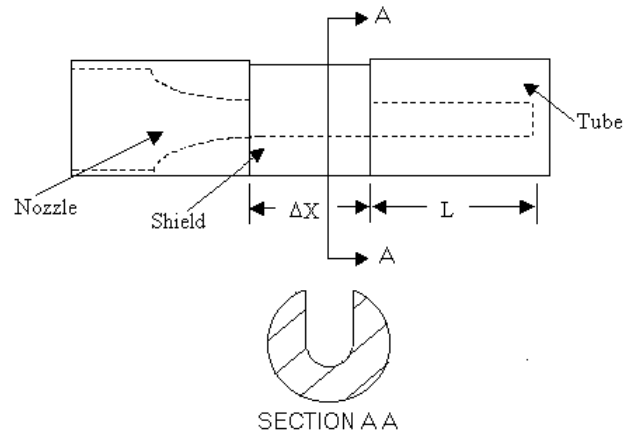


Figure 2: Schematic of HTFA used in the control experiments. The nozzle is on the left, the tube is on the right, and between them is the shield directing the flow into a focused location.

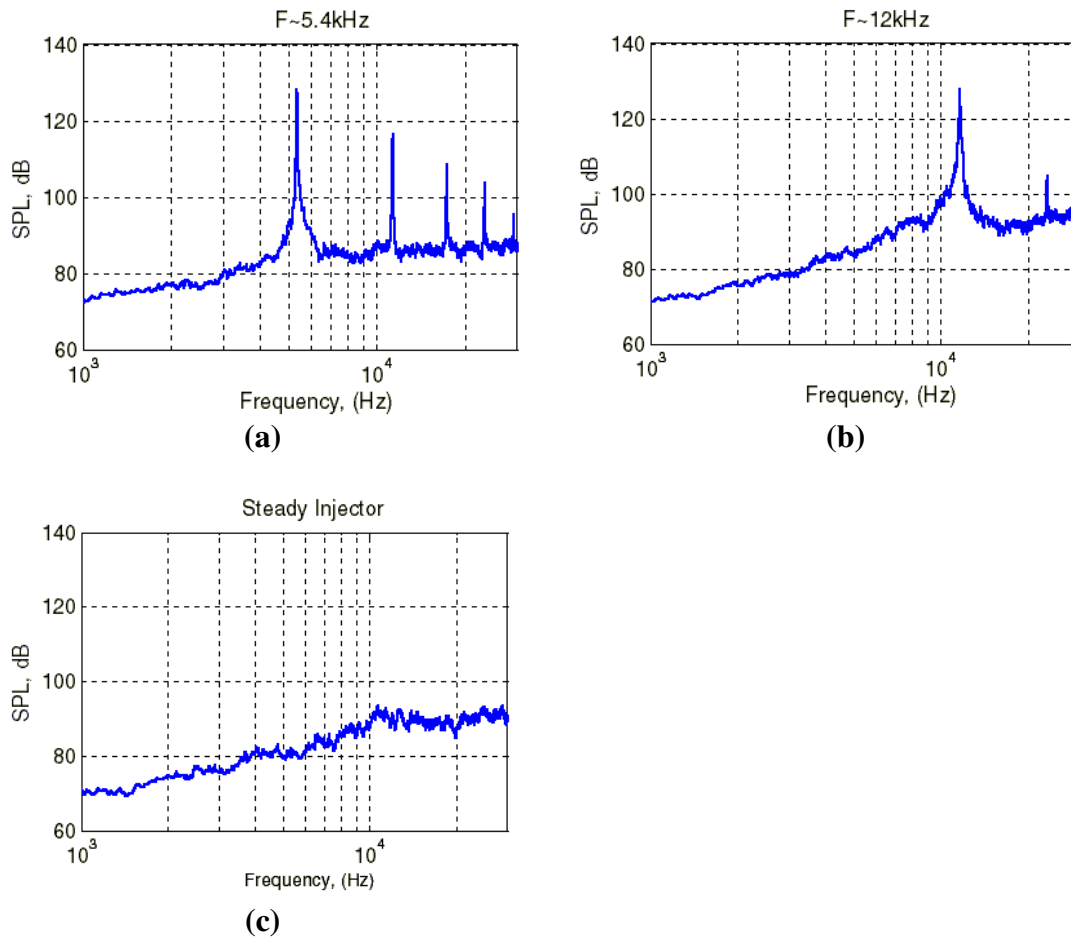


Figure 3: Far-field spectra of the three different actuators used in current work: (a) HTFA pulsating at 5.4 kHz; (b) HTFA pulsating at 12 kHz; (c) steady injector

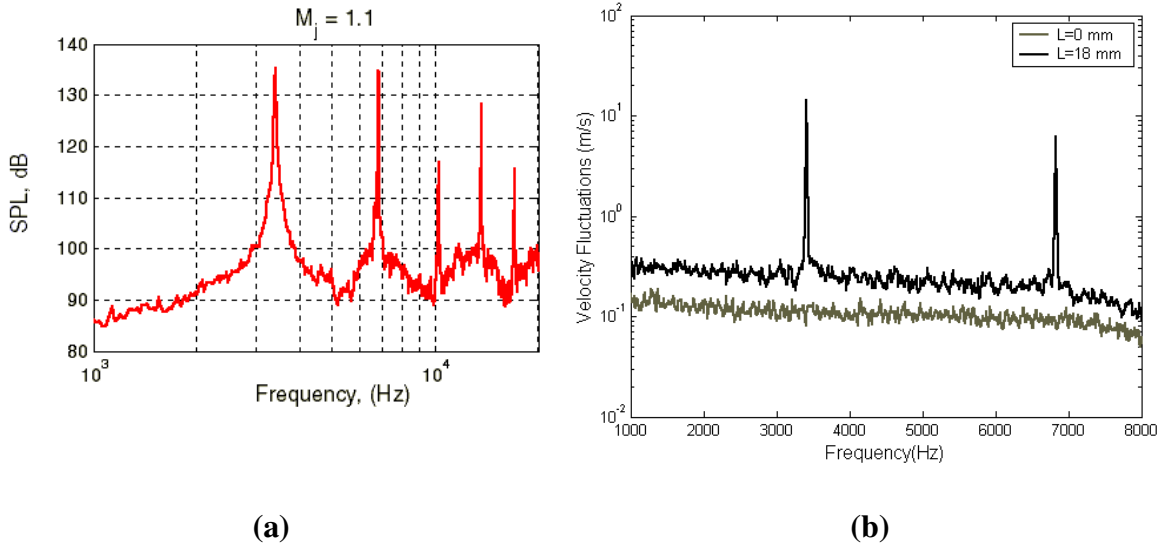


Figure 4: Comparison of far-field spectrum (a) and velocity fluctuations spectra at the exit of a HTFA with tube depth L of 18 mm and a plugged tube ($L = 0$ mm) (b).

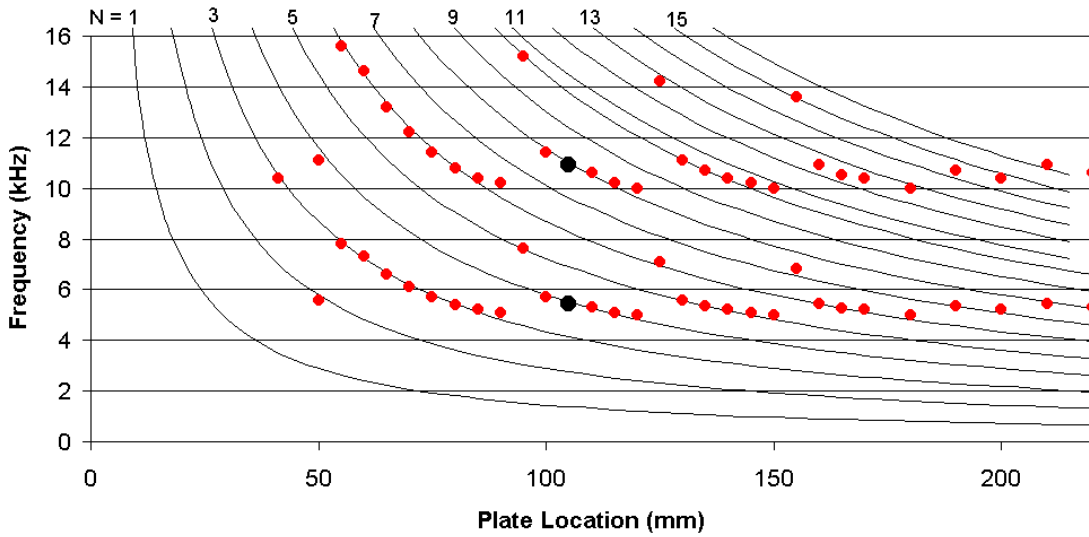


Figure 5: Impinging tone frequency versus plate location for the current experimental setup. Dots represent experimental data recorded in the far field by the microphone at $\phi = 80^\circ$. Solid lines represent the frequency predicted using Powell's formula.

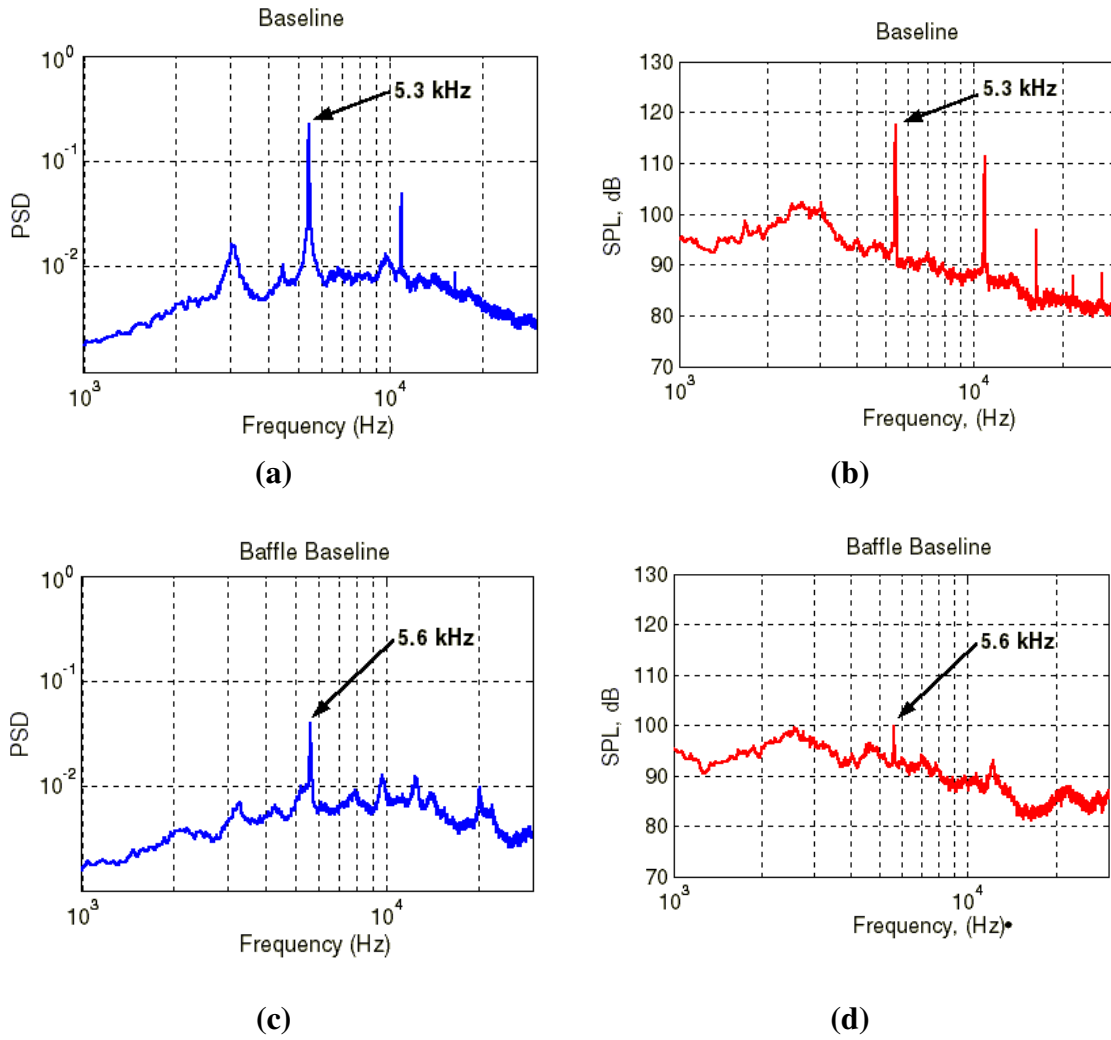


Figure 6: Spectra of the impinging jet without forcing: (a) baseline near-field; (b) baseline far-field; (c) baffled baseline near-field; (d) baffled baseline far-field.

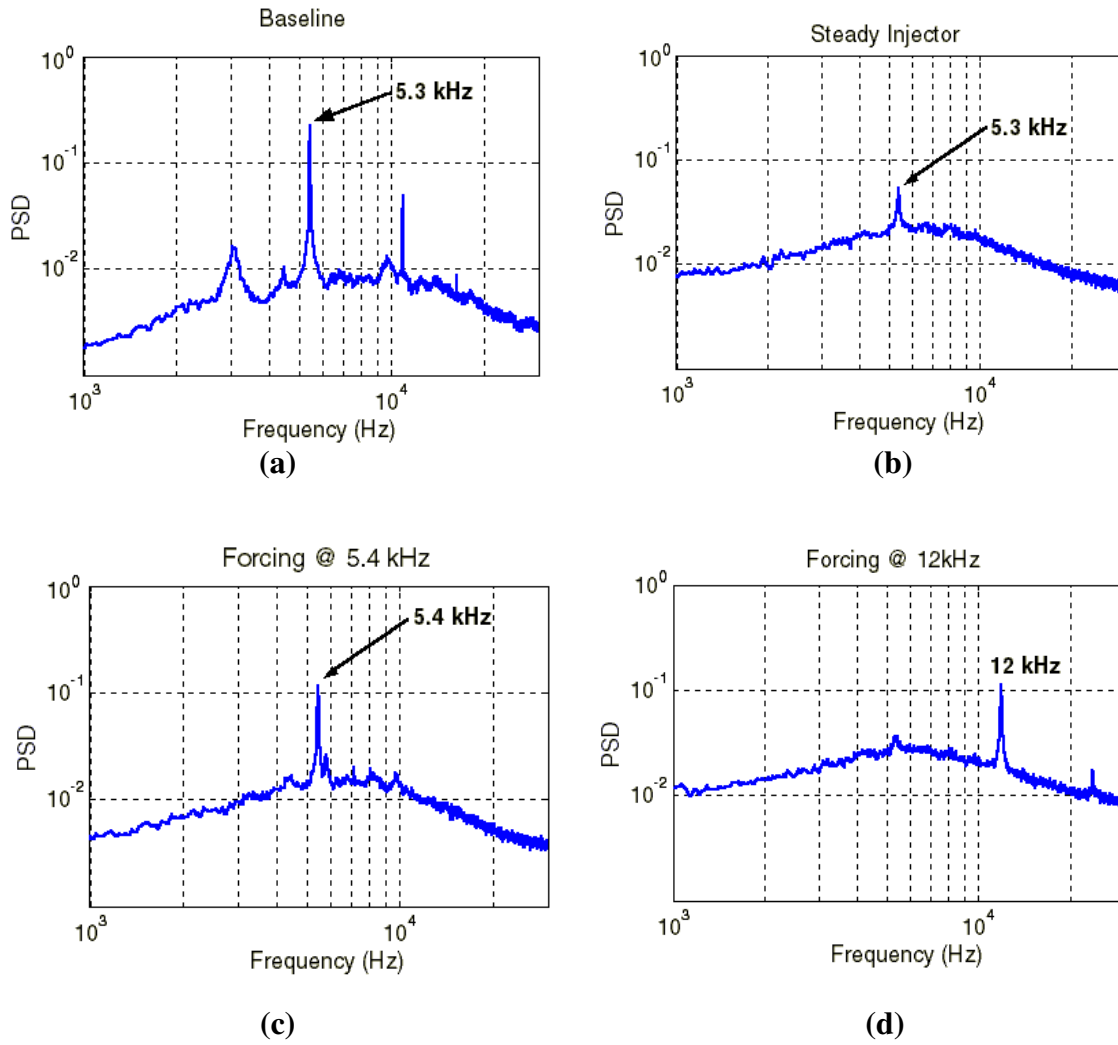


Figure 7: Near-field spectra at $\theta = 0^\circ$ of the baseline jet and the three forced jets: (a) baseline; (b) steady injection; (c) 5.4 kHz forcing; (d) 12 kHz forcing

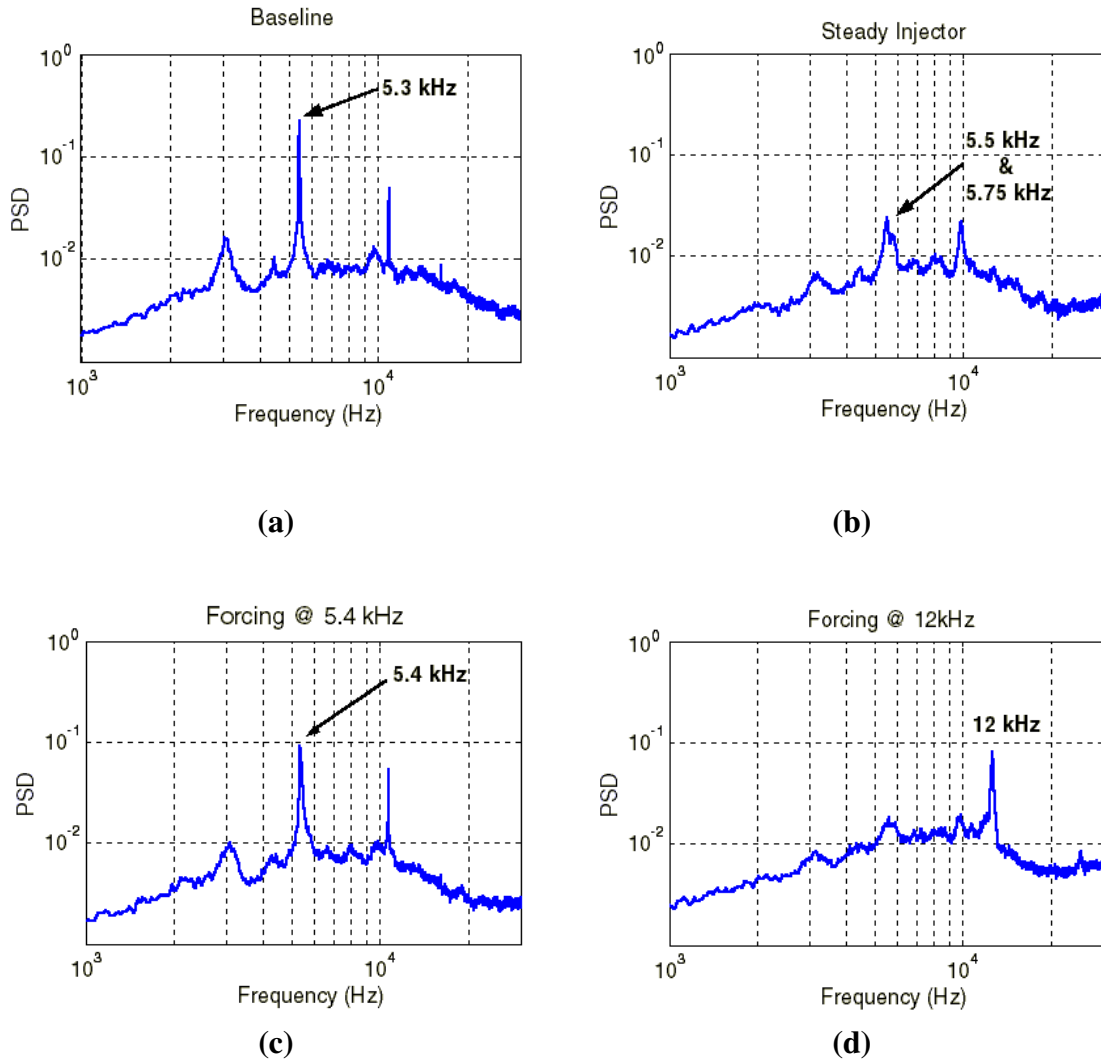


Figure 8: Near-field spectra at $\theta = 90^\circ$ of the baseline jet and the three forced jets: (a) baseline; (b) steady injection; (c) 5.4 kHz forcing; (d) 12 kHz forcing

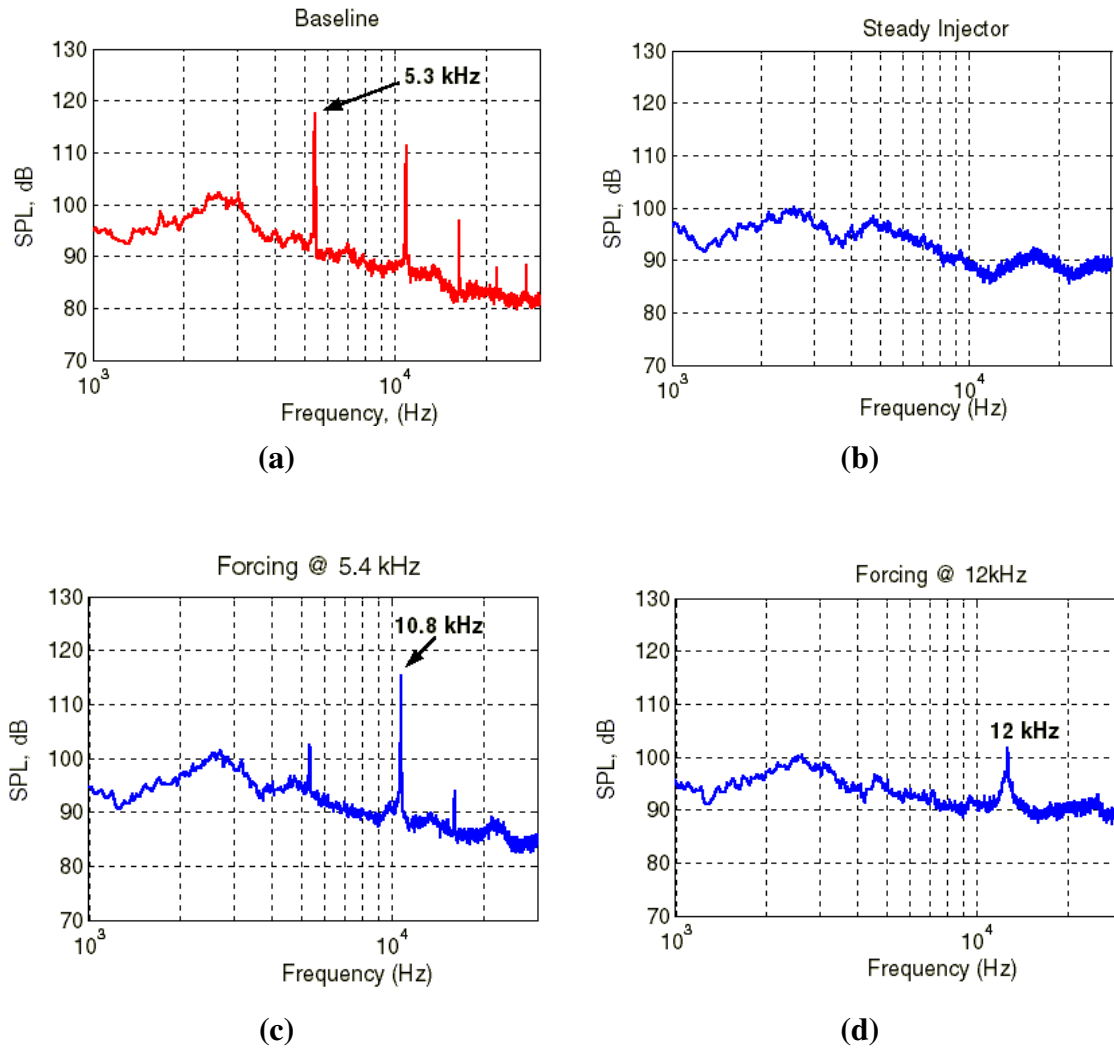


Figure 9: Far-field spectra at $\theta = 0^\circ$ of the baseline jet and the three forced jets:
 (a) baseline; (b) steady injection; (c) 5.4 kHz forcing; (d) 12 kHz forcing

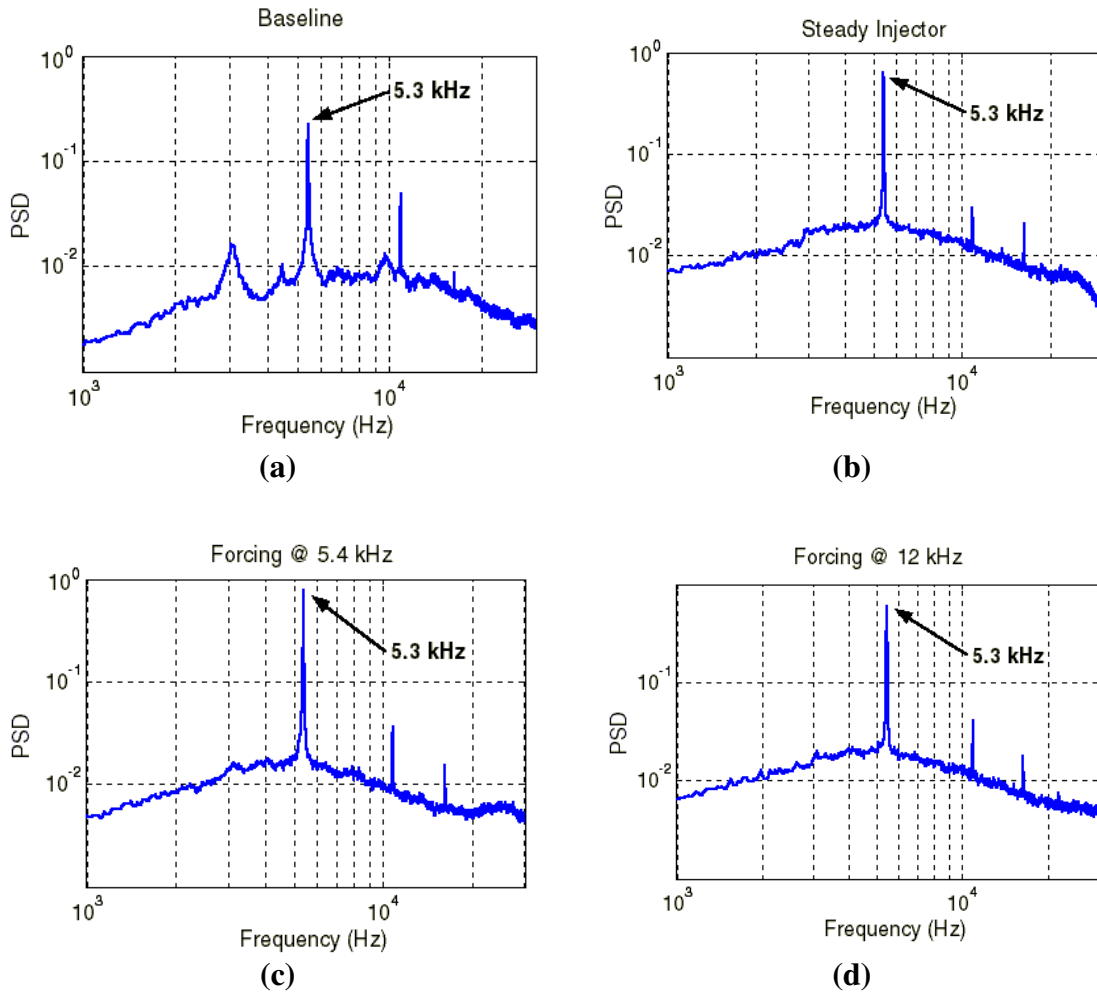


Figure 10: Near-field spectra at $\theta = 0^\circ$ of the baseline jet and the three forced jets: (a) baseline; (b) steady injection; (c) 5.4 kHz forcing; (d) 12 kHz forcing

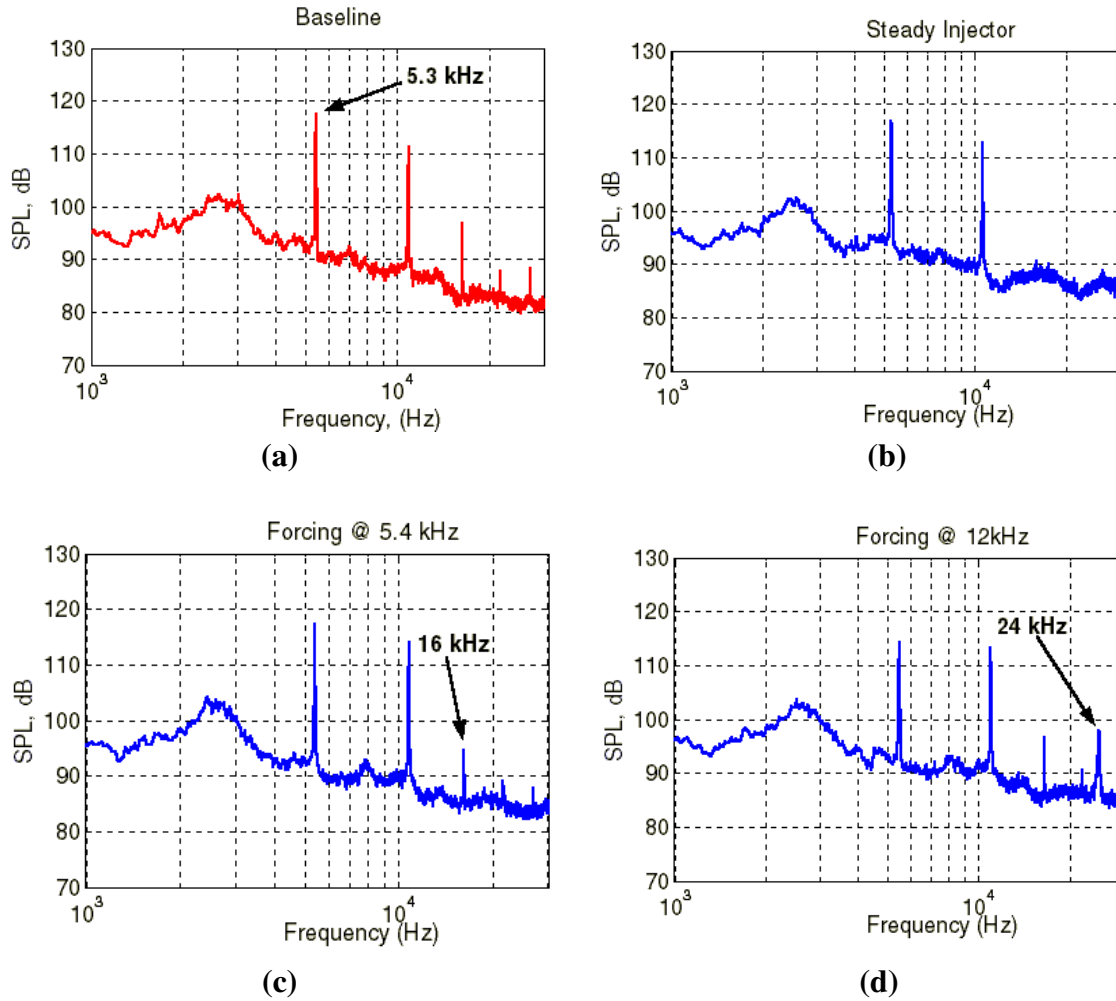


Figure 11: Far-field Near-field spectra at $\theta = 0^\circ$ of the baseline jet and the three forced jets:
 (a) baseline; (b) steady injection; (c) 5.4 kHz forcing; (d) 12 kHz forcing

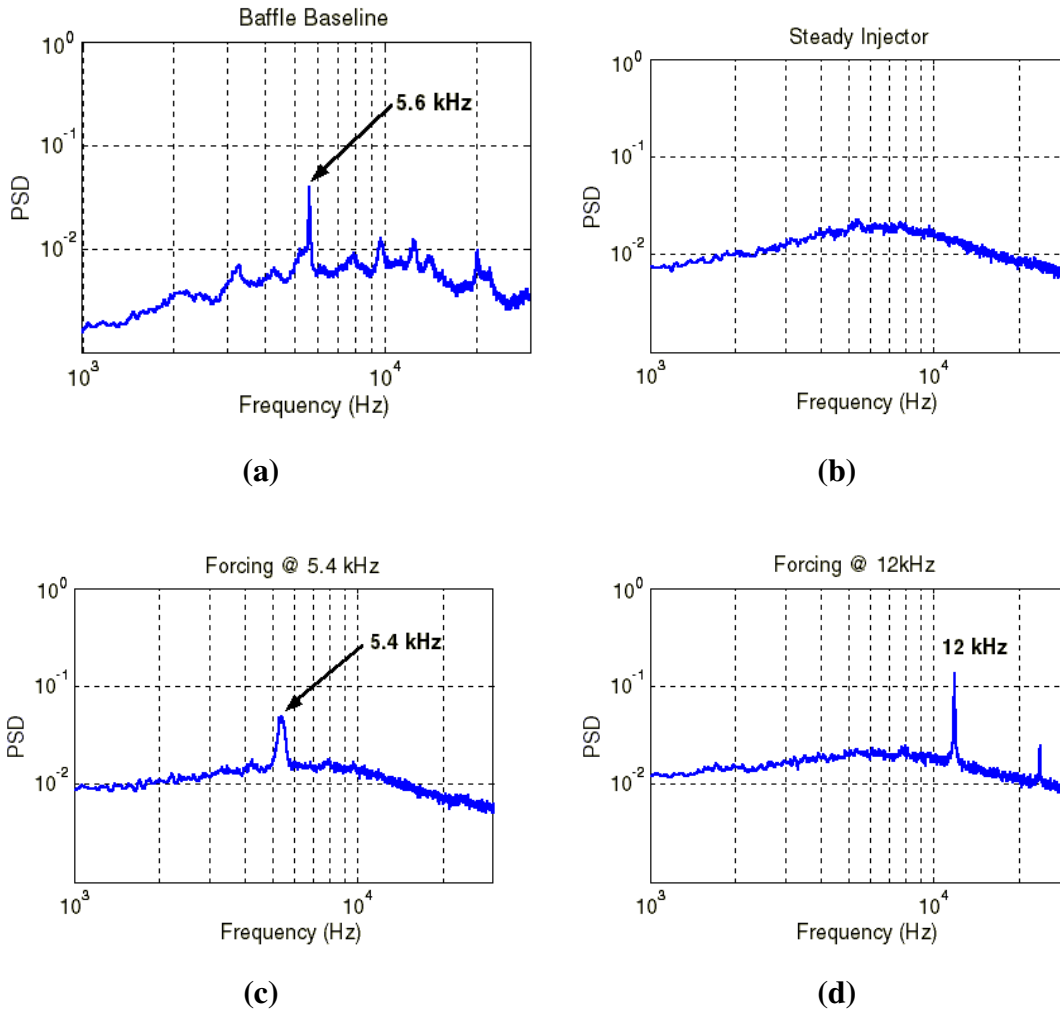


Figure 12: Near-field spectra at $\theta = 0^\circ$ of the baffled baseline jet and the three forced jets: (a) baseline; (b) steady injection; (c) 5.4 kHz forcing; (d) 12 kHz forcing

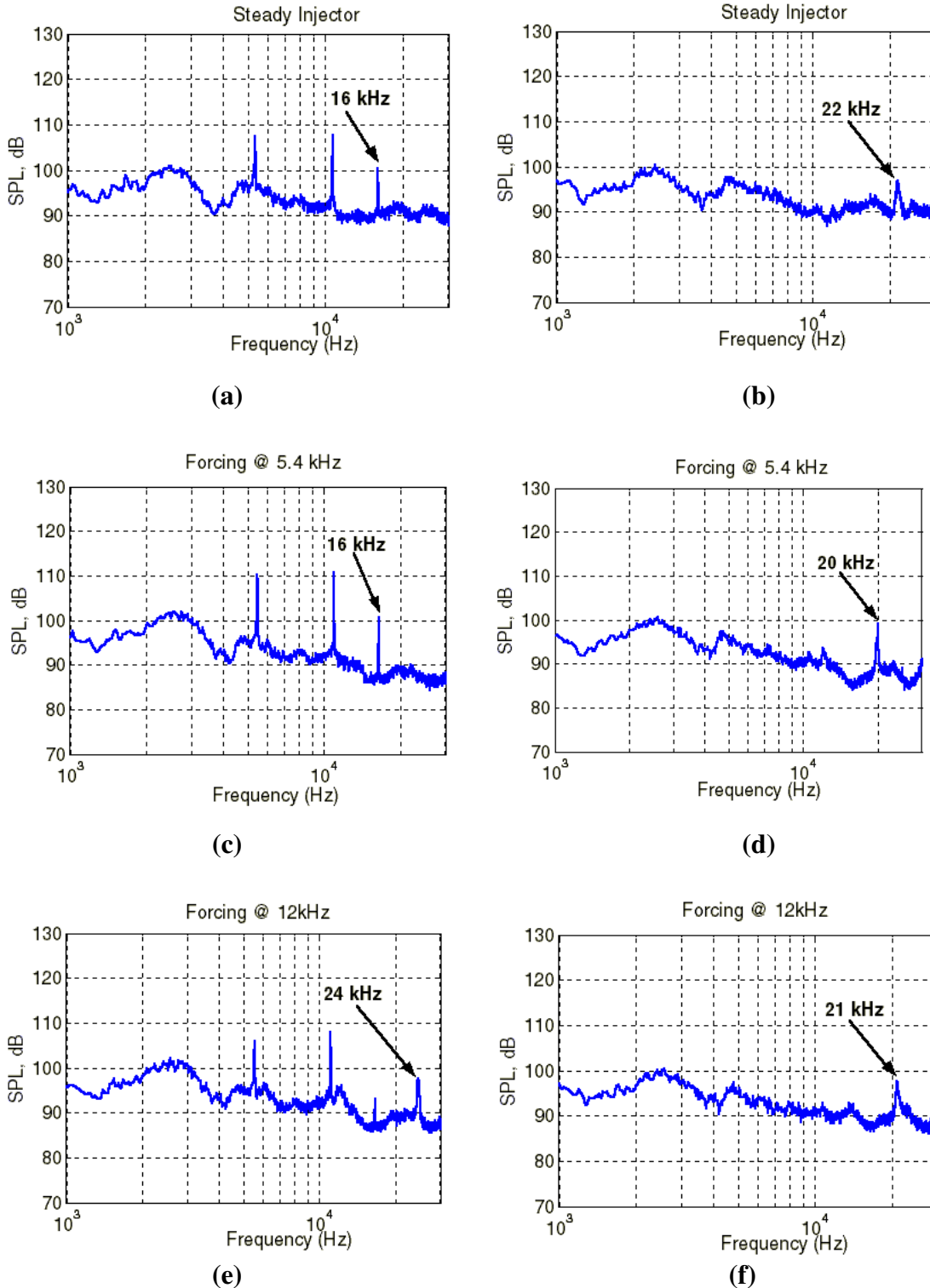


Figure 13: Far-field spectra at $\theta = 0^\circ$ of the baffled jet with one actuator: (a) steady injection on the same side of the baffle; (b) steady injection on the opposite side of the baffle; (c) 5.4 kHz forcing on the same side of the baffle; (d) 5.4 kHz forcing on the opposite side of the baffle; (e) 12 kHz forcing on the same side of the baffle; (f) 12 kHz forcing on the opposite side of the baffle